

## Article

# Ag/ZnO Thin Film Nanocomposite Membrane Prepared by Laser-Assisted Method for Catalytic Degradation of 4-Nitrophenol

Tahani A. Alrebdi <sup>1</sup>, Hoda A. Ahmed <sup>2,3</sup>, Fatemah H. Alkallas <sup>1</sup>, Rami Adel Pashameah <sup>4</sup>,  
Salhah H. Alrefae <sup>3</sup>, Emaan Alsubhe <sup>5</sup>, Ayman M. Mostafa <sup>6,7,\*</sup> and Eman A. Mwafy <sup>7,8</sup>

- <sup>1</sup> Department of Physics, College of Science, Princess Nourah bint Abdulrahman University, P.O. Box 84428, Riyadh 11671, Saudi Arabia; taalrebdi@pnu.edu.sa (T.A.A.); fhalkallas@pnu.edu.sa (F.H.A.)
- <sup>2</sup> Department of Chemistry, Faculty of Science, Cairo University, Cairo 12613, Egypt; ahoda@sci.cu.edu.eg
- <sup>3</sup> Chemistry Department, College of Sciences, Taibah University, Yanbu 30799, Saudi Arabia; srfaay@taibahu.edu.sa
- <sup>4</sup> Department of Chemistry, Faculty of Applied Science, Umm Al-Qura University, Makkah 24230, Saudi Arabia; rapasha@uqu.edu.sa
- <sup>5</sup> Physics Department, Faculty of Science, Taibah University, Yanbu 30799, Saudi Arabia; esobhe@taibahu.edu.sa
- <sup>6</sup> Spectroscopy Department, Physics Division Institute, National Research Centre, 33 El Bohouth St. (Former El Tahrir St.), Dokki, Giza 12622, Egypt
- <sup>7</sup> Laser Technology Unit, Center of Excellent for Advanced Science, National Research Centre, 33 El Bohouth St. (Former El Tahrir St.), Dokki, Giza 12622, Egypt; emanmwafynrc@gmail.com
- <sup>8</sup> Physical Chemistry Department, Advanced Materials Technology and Mineral Resources Research Institute, National Research Centre, Giza 12622, Egypt
- \* Correspondence: aymanmdarwish@gmail.com



**Citation:** Alrebdi, T.A.; Ahmed, H.A.; Alkallas, F.H.; Pashameah, R.A.; Alrefae, S.H.; Alsubhe, E.; Mostafa, A.M.; Mwafy, E.A. Ag/ZnO Thin Film Nanocomposite Membrane Prepared by Laser-Assisted Method for Catalytic Degradation of 4-Nitrophenol. *Membranes* **2022**, *12*, 732. <https://doi.org/10.3390/membranes12080732>

Academic Editor: Ahmed M. Khalil

Received: 11 July 2022

Accepted: 20 July 2022

Published: 24 July 2022

**Publisher's Note:** MDPI stays neutral with regard to jurisdictional claims in published maps and institutional affiliations.



**Copyright:** © 2022 by the authors. Licensee MDPI, Basel, Switzerland. This article is an open access article distributed under the terms and conditions of the Creative Commons Attribution (CC BY) license (<https://creativecommons.org/licenses/by/4.0/>).

**Abstract:** Zinc oxide thin film (ZnO thin film) and a silver-doped zinc oxide nanocomposite thin film (Ag/ZnO thin film) were prepared by the technique of the pulsed laser deposition at 600 °C to be applicable as a portable catalytic material for the removal of 4-nitrophenol. The nanocomposite was prepared by making the deposition of the two targets (Zn and Ag), and it was analyzed by different techniques. According to the XRD pattern, the hexagonal wurtzite crystalline form of Ag-doped ZnO NPs suggested that the samples were polycrystalline. Additionally, the shifting of the diffraction peaks to the higher angles, which denotes that doping reduces the crystallite size, illustrated the typical effect of the dopant Ag nanostructure on the ZnO thin film, which has an ionic radius less than the host cation. From SEM images, Ag-doping drastically altered the morphological characteristics and reduced the aggregation. Additionally, its energy band gap decreased when Ag was incorporated. UV spectroscopy was then used to monitor the catalysis process, and Ag/ZnO thin films had a larger first-order rate constant of the catalytic reaction  $K$  than that of ZnO thin film. According to the catalytic experiment results, the Ag/ZnO thin film has remarkable potential for use in environmentally-favorable applications.

**Keywords:** PLD; thin film; ZnO; nanocomposite; catalytic degradation; membrane

## 1. Introduction

Thin films are more useful structures to study than their bulk counterparts because of their versatility and positive characteristics. Thin-film assembly of surface-supported metal–metal oxides is becoming more and more ubiquitous, and this is expected to lead to new scientific discoveries as well as expanded application opportunities [1–5]. Examples of applications include membrane-based chemical species separation, silicon integration for electronic detection of volatile compounds, and electrochemical catalysis. ZnO can be considered as a one of the most important materials as it can be used in several application domains. Additionally, ZnO has great piezoelectric properties and exceptional chemical

stability due to its impressive semiconductor performance. Over the past few decades, ZnO thin films have been the subject of substantial research [5–8]. It has a number of clearly stated benefits, including being affordable, plentiful, safe to use, chemically stable, very transparent in the visible and near-infrared spectral area, ecologically benign, and highly catalytic. Since ZnO has a direct bandgap, it offers special features and the versatility to be employed in a variety of applications, including LEDs, gas sensors, optoelectronic components, UV lasers, solar cells, and screen displays [9–13].

The nanocomposite semiconductor thin film is formed by doping the semiconductor thin film with another thin film or metallic nanoparticles, which helps to enhance the optoelectronic properties. These materials provide ZnO with n-type conductivity because the presence of oxygen vacancies leads to the creation of  $\text{Zn}^{+2}$  interstitials. However, it can be doped to achieve P-type conductivity, making it promising for use in research. According to theoretical research, silver and gold are an appropriate dopant to obtain P-type ZnO. Ag is the most suitable choice among all of the transition metals due to its solubility and the fact that it contains one outermost electron, which accounts for its huge ionic size and orbital energy. In addition, compared to other transition metals, Ag is a cheap, non-toxic, superior electrical and high thermal conductor. The main reason for choosing ZnO doped with Ag is because it improves the characteristics and hinders the trapping of photo-generated electrons, which lengthens the lifespan of charge-separated states [14–18].

The pulsed laser deposition technique (PLD) has been found to be the most efficient and quick method for producing stoichiometric thin film by utilizing multiple targets; these are appealing qualities that make it possible to produce multi-component thin films of high quality. Thin films of metal oxide and other materials related to metal oxide are routinely produced using PLD. Metal nanoparticle-doped oxide films have recently been demonstrated to possess intriguing characteristics such as significant nonlinearity, photocatalysis, etc. [19–22].

Herein, we synthesized ZnO thin film and developed this structure by embedding the structure with Ag nanostructure to form Ag-doped ZnO nanocomposite thin films by PLD to apply in water treatment. The novelty in this work was based on filling vacancies in the zinc matrix and interstitial zinc atoms with Ag atoms. Different techniques were used to investigate the prepared thin films and determine the changes in their characteristics. Then, the prepared films were used as catalytic-degradable material for the water purification field.

## 2. Experimental Work

### 2.1. Materials

Merck supplied the 4-nitrophenol (4-NP), zinc dust target (Zn), silver target (Ag), sodium borohydride ( $\text{NaBH}_4$ ), and mono-crystalline quartz substrate ( $4 \times 1 \times 0.1 \text{ cm}^3$ ), which was washed by chromic acid (purchased from Nasr, Egypt) and then thoroughly rinsed with distilled water, followed by sonication in an ultrasonic bath for 30 min. After treatment, the slides were stored in water until required for use.

### 2.2. Preparation Method

As previously reported, to adjust the optimum condition of dual-pulsed laser deposition [23–25], the thin film was created via PLD of the metal target at the following specifications: 600 °C reaction temperature, 7 ns pulse duration, 1064 nm wavelength, 30 min ablation time, and 7.5 W average power. As shown in Figure 1, pulsed laser ablation was first performed on the Zn to create ZnO thin films on quartz substrate, then on the Ag to create Ag/ZnO nanocomposite thin films on quartz substrate. For Ag-doped ZnO thin film, the film thickness was determined using a profilometer (SurfTestSJ-301) and was found to be 300 nm for ZnO thin film and 500 nm for Ag/ZnO thin film.

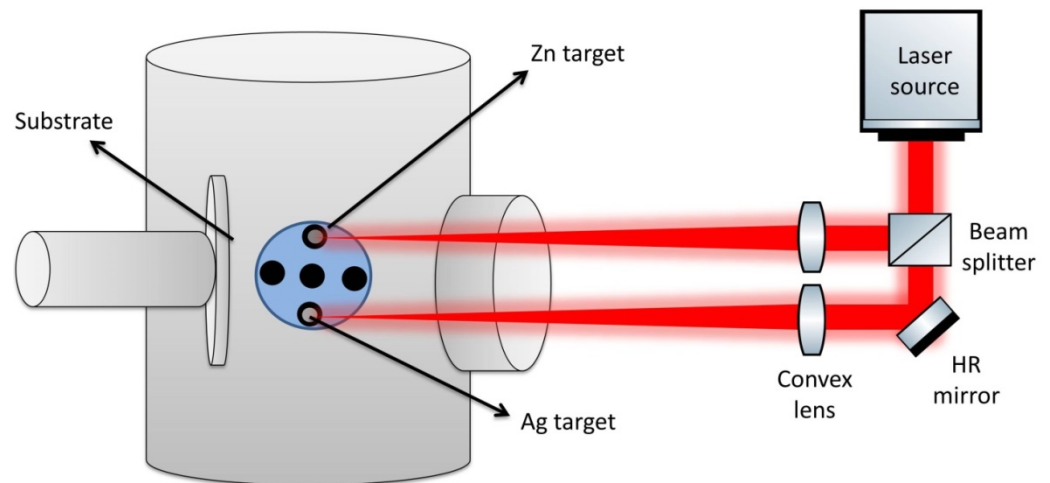


**Figure 1.** Representative graph of the preparation thin film of Ag/ZnO by PLD.

### 2.3. Characterization Techniques

UV-visible spectrophotometer (JASCO 570 UV-Vis, Japan), X-ray diffraction (XRD, Shimadzu 7000, Japan), scanning electron microscopic and energy dispersive X-ray (SEM-EDX, Quanta FEG 250, FEI, Czech Republic), and photoluminescence Spectrometer (PL, JASCO, FP-6500, Japan) were used for the characterization.

### 2.4. Catalytic Removal Procedure of 4-NP

The catalytic degradation procedure was conducted by adding the following items together: 100  $\mu\text{L}$  of 0.1 M  $\text{NaBH}_4$  (reducing agent), 2.77 mL of 0.4 mM 4-NP (pollutant) and the prepared thin films were used as a catalytic degradable material. Then, the UV-visible spectrum was examined every 10 min in order to examine the catalytic reaction.

## 3. Results

### 3.1. Investigation of the Prepared Films

Figure 2 shows the diffractogram of ZnO thin film and its embedding with Ag thin films to create a nanocomposite structure thin film. For ZnO thin film, a number of diffraction peaks that appeared corresponded to the reflection planes (1 0 0), (0 2 2), (1 0 2), (1 1 0), (1 0 3), (2 0 0), (1 1 2), and (2 0 1), which is an exact match to the XRD diffraction pattern of pure ZnO (JCPDS card No. 80-0075) [26]. There are no phases that matched any other oxides other than ZnO, which can be seen in the diffractogram for ZnO thin films. Additionally, the diffractogram of the prepared ZnO thin film has a prominent ZnO (0 0 2) peak, indicating that the films are oriented with the c-axis normal to the substrate with a high intensity peak and a sharp shape. In another words, for the ZnO thin film embedded with Ag nanostructure, three XRD peaks of the (1 1 1), (2 0 0), and (2 2 0) planes were indexed to silver, which was fcc phase-matched, confirming Ag as the secondary phase based on the JCPDS card No. 04-0783 [27]. Additionally, the Scherrer formula was used to determine the crystalline size for the (1 0 1) plane, the highest characteristic peak [28,29].

$$D = \frac{(0.9)\lambda}{\beta \cos\theta}$$

where  $\lambda$  is the wavelength of X-ray 1.54  $\text{\AA}$ ,  $\beta$  is FWHM and  $\theta$  is the diffraction angle of the (1 0 1) plane. The crystallite size decreases from 42 to 19 nm as the Ag dopant concentration increases. As the amount of Ag dopant in thin films increases, the lattice strain between crystallites also increases. More Ag ions cause the lattice to become disordered, which results in a reduction in crystallite size. Because  $\text{Ag}^+$  ions have a higher radius (0.126 nm) than  $\text{Zn}^{2+}$  ions, the lattice constants rise, increasing the cell volume (0.074 nm).

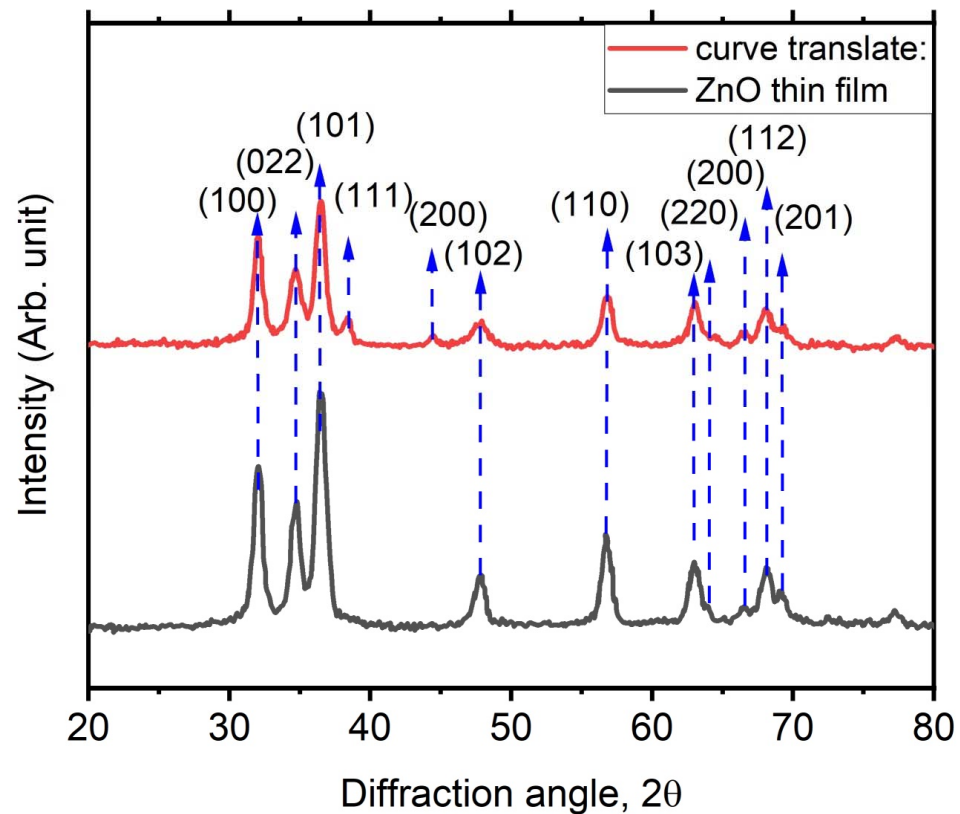


**Figure 2.** XRD diffractogram of ZnO thin film before and after being embedded with Ag thin films.

Figure 3 displays SEM images of the annealed ZnO and annealed ZnO/Ag films. The pulsed laser deposition of undoped ZnO films typically results in dense films. It was clear that in the case of Ag-doped films, bright spots started to appear, which is related to the embedding of the ZnO thin film with Ag film. Moreover, the ZnO/Ag thin films' elemental composition was examined using EDX spectra to establish the presence of Ag. A typical EDX result for thin films is shown in Figure 3. No other components were found, and the top concentrations were Zn, O, and Ag, which was confirmed by elemental mapping.

UV-vis spectrophotometer was used to evaluate the varying in the optical properties of the prepared structure. Figure 4 displays the UV-vis optical absorption spectra of ZnO and Ag/ZnO thin films. Strong excitonic peaks with significant absorbance strength are visible in the sample at 372 nm (pure ZnO). In addition, compared to pure ZnO, the absorption edge shifted to a longer wavelength with Ag deposition to create Ag/ZnO thin films. The inclusion of Ag into the ZnO matrix may be responsible for this shift in the absorption edge. Particles in doped ZnO may be smaller than the exciton Bohr radius, according to a shift in the absorption spectra [30–32]. This decrease in the transmittance values of the Ag/ZnO thin film in comparison to ZnO thin film may be caused by grain boundary scattering and the visible light absorption caused by surface plasmon resonance (SPR), which is in excellent agreement with previous studies in the literature [33,34].



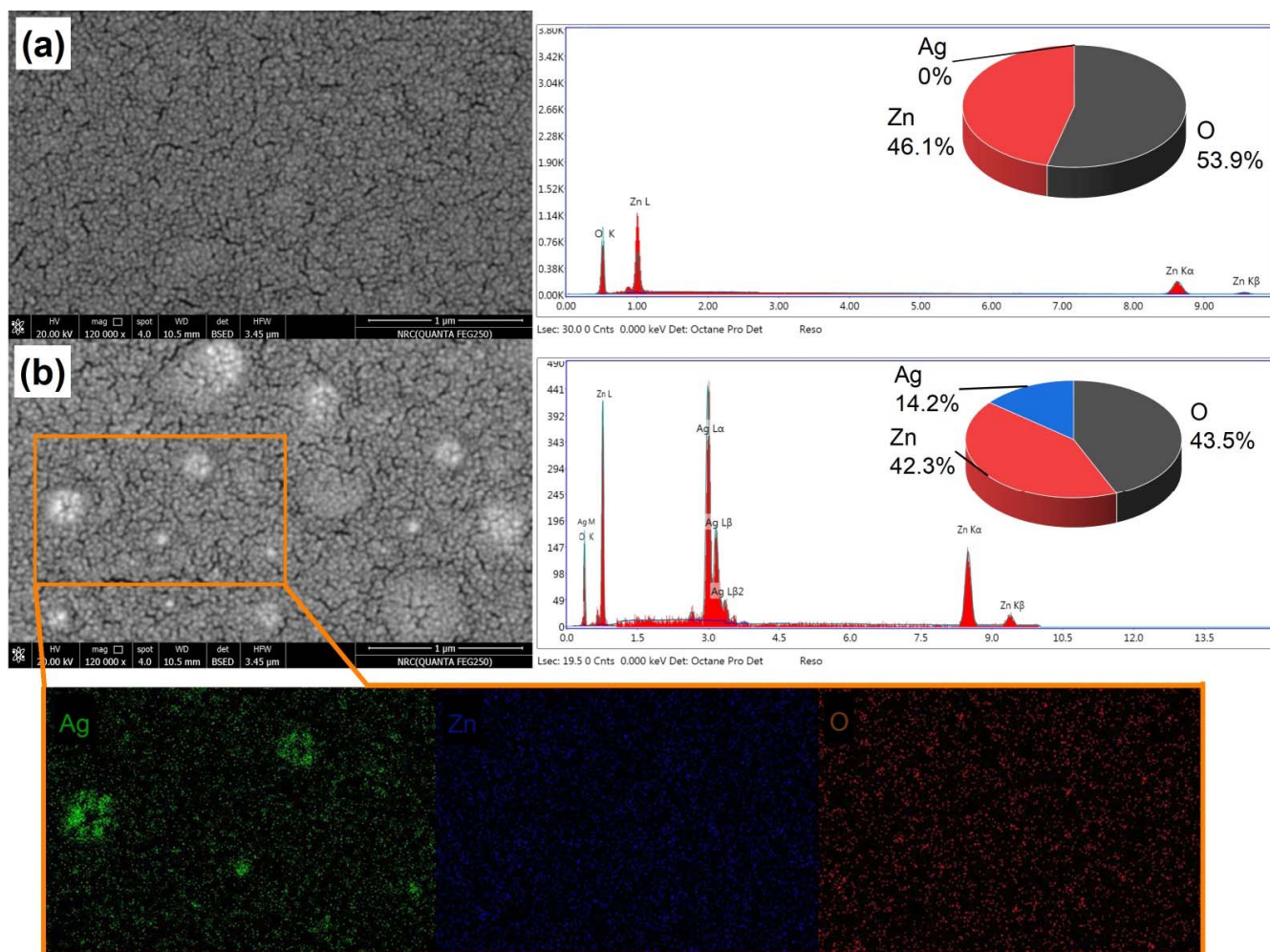


Figure 3. SEM image and elemental analysis of the prepared thin films of (a) ZnO and (b) Ag/ZnO.

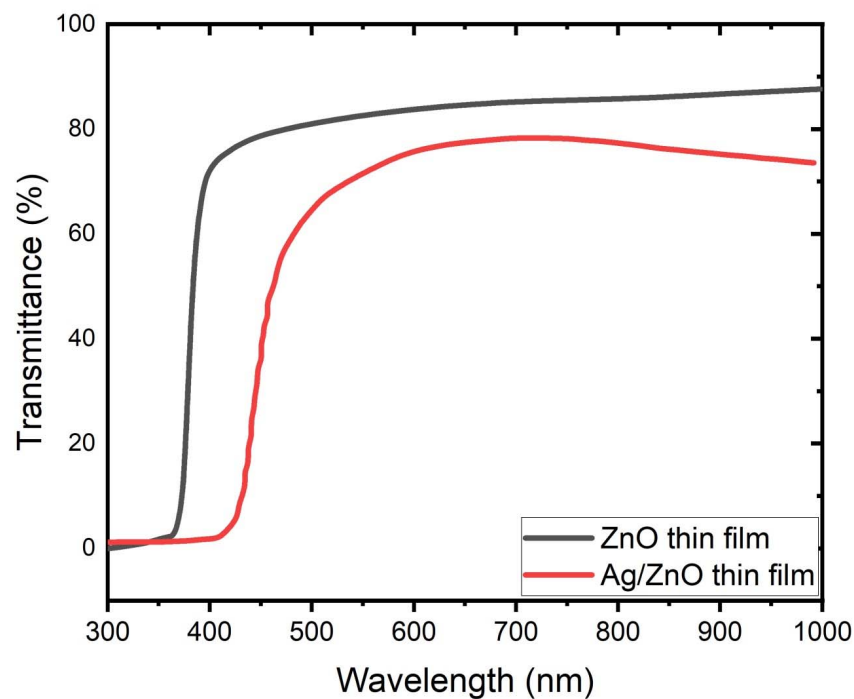
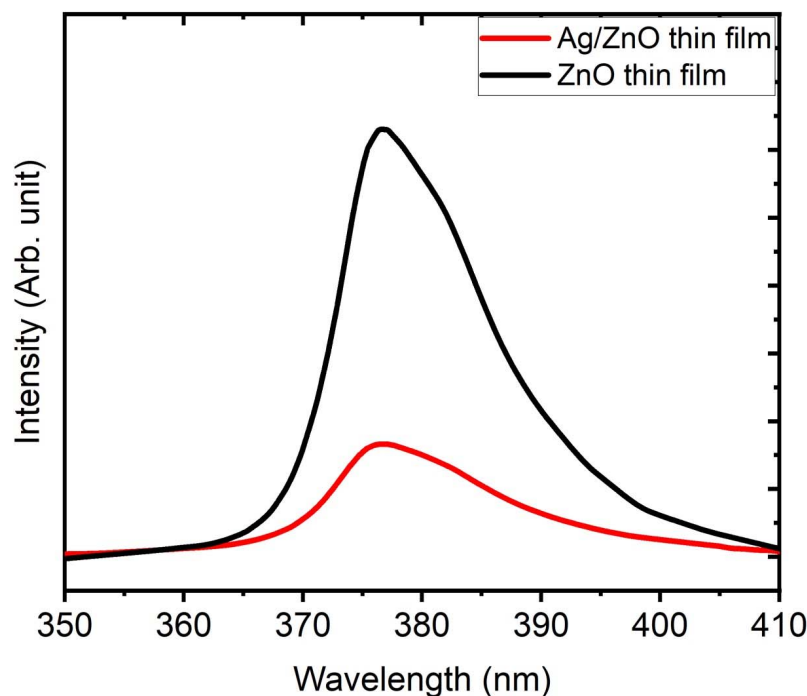


Figure 4. Absorbance spectra of ZnO thin film before and after being embedded with Ag thin films.

Figure 5 displays the PL spectra of thin films, which were calculated using an excitation wavelength of 325 nm and an emission spectrum that ranged from 360 to 410 nm. The samples' PL spectra show a single violet luminescence peak with a center wavelength of 378 nm. It has been reported that thin ZnO films produced on quartz via PLD emit violet fluorescence, which represents a mixture from the oxygen or zinc vacancies. In other words, in the case of Ag/ZnO nanocomposite thin film, the interface traps between Ag nanoclusters and ZnO grains that exist at the grain boundaries generate violet light from the electronic transition between CB and VB. Additionally, the emission spectra showed a substantial violet emission at 382 nm, which was probably generated by radiate defects brought on by interface traps at the grain boundaries. After Ag was added, this band edge emission peak migrated slightly to a higher value, indicating that the optical bandgap had shrunk. Besides, the presence of oxygen vacancies that interacted with Ag doping also had an impact on the location and intensity of this PL emission. Since  $\text{Ag}^{2+}$  ions take the position of  $\text{Zn}^{2+}$  ions in the high concentration of Ag-doped ZnO, the peak's intensity is lower than it is for pure ZnO [35–38].



**Figure 5.** PL spectra of ZnO thin film before and after being embedded with Ag thin films.

### 3.2. Catalytic Activity

Then, using the UV-visible spectra in Figure 6, the catalyst's catalytic capabilities for reducing 4-NP in an excess of  $\text{NaBH}_4$  were examined. The reduction of 4-NP in the presence of  $\text{NaBH}_4$  at 298 K was catalyzed by the prepared thin films, as seen in the UV spectrum in Figure 6. The absorption of 4-NP was characterized via two peaks (314 nm and 400 nm) while the absorption characteristic peak of 4-NP ion was characterized by one peak (403 nm), and the absorption characteristic peak of the conversion from 4-NP to 4-AP was characterized by one peak (300 nm). This was related to four processes that took place in the catalytic reduction of 4-NP: (1) adsorption of the reactant 4-NP onto the thin ZnO or Ag/ZnO surface; (2) diffusion of 4-NP to the active site; (3) reduction on the site by  $\text{NaBH}_4$ ; and (4) desorption of the product [39]. According to the UV-vis spectrum, ZnO thin films have a marginal catalytic effect in the first 20 min with an efficiency that does not exceed 35%, whereas Ag/ZnO thin films demonstrate excellent adsorption of 4-NP in the initial period of time with an efficiency that exceeds 90% [40–42].

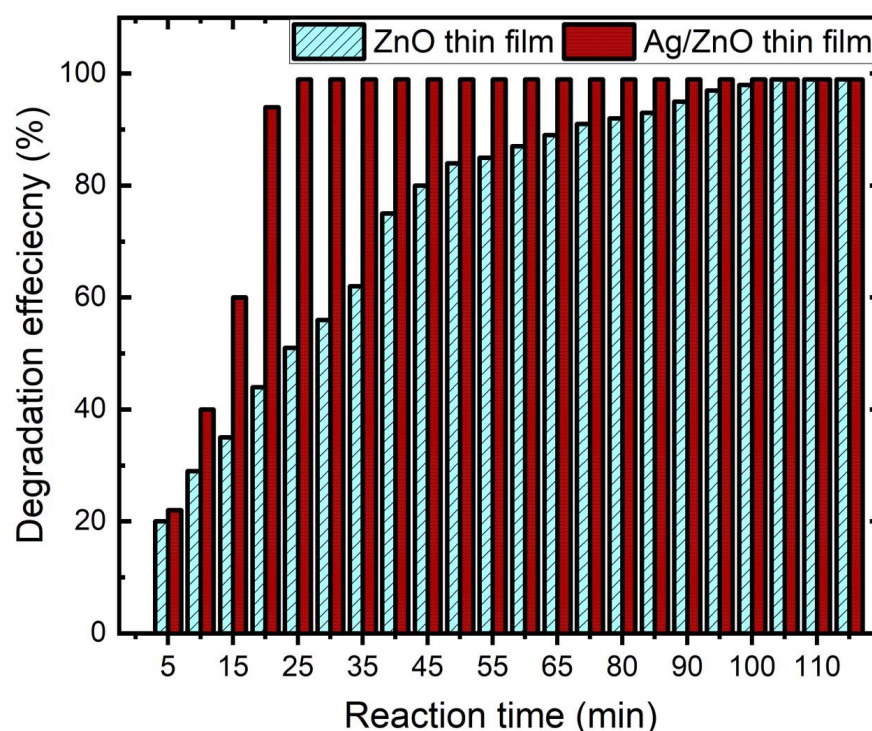


**Figure 6.** Degradation efficiency of ZnO thin film before and after being embedded with Ag thin films against 4-NP.

We inserted a single strip of the prepared thin film ( $1\text{ cm} \times 2\text{ cm}$ ) into a solution of deionized water containing 4-NP and  $\text{NaBH}_4$  at 298 K in order to compare the catalytic effects of the ZnO and Ag/ZnO thin films. Figure 6 shows the degradation efficiency for ZnO thin film and Ag/ZnO thin film against the reaction process. As can be seen, the Ag/ZnO thin film completed the conversion of 4-NP to 4-AP in at least 27 min, whereas the ZnO thin film completed it in 105 min. The catalytic reaction took place after the catalyst accepted the electron donor  $\text{BH}_4^-$ , transferred it to the electron acceptor 4-NP, and then allowed it to proceed. It might be argued that the rate of decrease was independent of the  $\text{NaBH}_4$  content because there was an overabundance of  $\text{NaBH}_4$ . The solution's color changed from light yellow-green to dark yellow-green when  $\text{NaBH}_4$  was added to create a 4-NP ion.

According to Figure 7, which shows the relationship of  $\ln(A_t/A_0)$  versus time ( $t$ ), the reaction showed a pseudo first-order reaction based on their linear correlation, where  $A_t$  and  $A_0$  are the absorbance values at the times (any time, zero time), respectively. The pseudo 1st rate constant of the Ag/ZnO thin film was significantly greater than that of the ZnO thin film. One of the reasons was that the Ag/ZnO structures produced better mass transfer than ZnO structure-assisted catalysts.

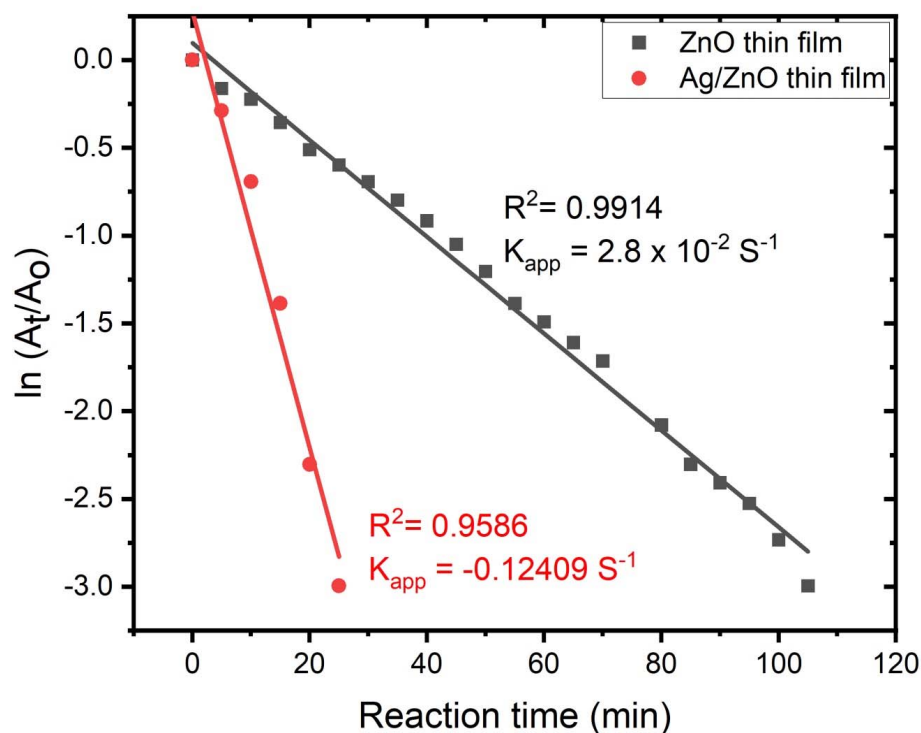


**Figure 7.** Investigation of  $\ln(A_t/A_0)$  with respect to reaction time ( $t$ ) for the thin films (ZnO and Ag/ZnO) against 4-NP.

#### 4. Conclusions

In conclusion, Ag-nanocluster-doped ZnO films were produced at 600 °C by PLD. Several analytical techniques were utilized to examine the produced thin films' physico-chemical characteristics in order to learn more about their optical, structural, and morphological characteristics. These methods revealed the crystalline structure, excellent surface homogeneity, and the production of nano-structural particle size in both the produced films. Then, ZnO structure and the Ag/ZnO structure were investigated for the removal of 4-NP, it was discovered that the degradation efficiency of the Ag/ZnO thin film completed the conversion to 4-AP in at least 27 min, whereas the ZnO thin film completed it in 105 min.

**Author Contributions:** Conceptualization, T.A.A.; methodology, S.H.A., A.M.M., E.A., T.A.A., E.A.M. and F.H.A.; formal analysis, A.M.M., E.A.M. and H.A.A.; investigation, A.M.M., S.H.A., E.A. and E.A.M.; resources, T.A.A., A.M.M., R.A.P. and F.H.A.; data curation, H.A.A.; writing—original draft preparation, R.A.P. and H.A.A.; writing—review and editing, E.A.M.; supervision, A.M.M.; project administration, A.M.M. and T.A.A.; funding acquisition, T.A.A. All authors have read and agreed to the published version of the manuscript.

**Funding:** This research was funded by the Princess Nourah bint Abdulrahman University Researchers Supporting Project number (PNURSP2022R71), Princess Nourah bint Abdulrahman University, Riyadh, Saudi Arabia.

**Acknowledgments:** The authors extend their sincere appreciation to Princess Nourah bint Abdulrahman University Researchers Supporting Project number (PNURSP2022R71), Princess Nourah bint Abdulrahman University, Riyadh, Saudi Arabia. The authors would also like to thank the Deanship of Scientific Research at Umm Al-Qura University for supporting this work with Grant Code: (22UQU4320141DSR37).

**Conflicts of Interest:** The authors declare no conflict of interest.



## References

1. Ahmad Fahri, M.A.S.; Rohizat, N.S.; Yudianta, A.; Fauzia, V.; Abdul Khudus, M.I.M.; Zakaria, R. Nonlinear optical response of zinc oxide nanorods with gold and silver alloy embedment. *Phys. B Condens. Matter* **2022**, *637*, 413899. [[CrossRef](#)]
2. Soudi, J.; Sandeep, K.M.; Sarojini, B.K.; Patil, P.S.; Maidur, S.R.; Balakrishna, K.M. Thermo-optic effects mediated self focusing mechanism and optical power limiting studies of ZnO thin films deposited on ITO coated PET substrates by RF magnetron sputtering under continuous wave laser regime. *Optik* **2021**, *225*, 165835. [[CrossRef](#)]
3. Seol, W.; Anoop, G.; Park, H.; Shin, C.W.; Lee, J.Y.; Kim, T.Y.; Kim, W.S.; Joh, H.; Samanta, S.; Jo, J.Y. Ferroelectricity in solution-processed V-doped ZnO thin films. *J. Alloys Compd.* **2021**, *853*, 157369. [[CrossRef](#)]
4. Mostafa, A.M. The enhancement of nonlinear absorption of Zn/ZnO thin film by creation oxygen vacancies via infrared laser irradiation and coating with Ag thin film via pulsed laser deposition. *J. Mol. Struct.* **2021**, *1226*, 129407. [[CrossRef](#)]
5. Mostafa, A.M. Preparation and study of nonlinear response of embedding ZnO nanoparticles in PVA thin film by pulsed laser ablation. *J. Mol. Struct.* **2021**, *1223*, 129007. [[CrossRef](#)]
6. Alkallas, F.H.; Ahmed, H.A.; Pashameah, R.A.; Alrefae, S.H.; Toghan, A.; Trabelsi, A.B.G.; Mostafa, A.M. Nonlinearity enhancement of Multi-walled carbon nanotube decorated with ZnO nanoparticles prepared by laser assisted method. *Opt. Laser Technol.* **2022**, *155*, 108444. [[CrossRef](#)]
7. ElFaham, M.M.; Mostafa, A.M.; Mwafy, E.A. The effect of reaction temperature on structural, optical and electrical properties of tunable ZnO nanoparticles synthesized by hydrothermal method. *J. Phys. Chem. Solids* **2021**, *154*, 110089. [[CrossRef](#)]
8. Upadhya, K.; Deekshitha, U.G.; Antony, A.; Ani, A.; Kityk, I.V.; Jedryka, J.; Wojciechowski, A.; Ozga, K.; Poornesh, P.; Kulkarni, S.D.; et al. Second and third harmonic nonlinear optical process in spray pyrolysed Mg: ZnO thin films. *Opt. Mater.* **2020**, *102*, 109814. [[CrossRef](#)]
9. Mostafa, A.M.; Mwafy, E.A.; Toghan, A. ZnO nanoparticles decorated carbon nanotubes via pulsed laser ablation method for degradation of methylene blue dyes. *Colloids Surf. A Physicochem. Eng. Asp.* **2021**, *627*, 127204. [[CrossRef](#)]
10. Alamro, F.S.; Toghan, A.; Ahmed, H.A.; Mostafa, A.M.; Alakhras, A.I.; Mwafy, E.A. Multifunctional leather surface embedded with zinc oxide nanoparticles by pulsed laser ablation method. *Microsc. Res. Tech.* **2022**, *85*, 1611–1617. [[CrossRef](#)]
11. Alturki, A.M. Effect of Preparation Method on the Particles Size, Dielectric Constant and Antibacterial Properties of ZnO Nanoparticles and Thin Film of ZnO/Chitosan. *Orient. J. Chem.* **2018**, *34*, 548. [[CrossRef](#)]
12. Edison, D.J.; Nirmala, W.; Kumar, K.D.A.; Valanarasu, S.; Ganesh, V.; Shkir, M.; AlFaify, S. Structural, optical and nonlinear optical studies of AZO thin film prepared by SILAR method for electro-optic applications. *Phys. B Condens. Matter* **2017**, *523*, 31–38. [[CrossRef](#)]
13. Alamro, F.S.; Mostafa, A.M.; Ahmed, H.A.; Toghan, A. Zinc oxide/carbon nanotubes nanocomposite: Synthesis, characterization and catalytic reduction of 4-nitrophenol via laser assistant method. *Surf. Interfaces* **2021**, *26*, 101406. [[CrossRef](#)]
14. Alamro, F.S.; Mostafa, A.M.; Al-Ola, K.A.A.; Ahmed, H.A.; Toghan, A. Synthesis of Ag Nanoparticles-Decorated CNTs via Laser Ablation Method for the Enhancement the Photocatalytic Removal of Naphthalene from Water. *Nanomaterials* **2021**, *11*, 2142. [[CrossRef](#)]
15. Mostafa, A.M.; Mwafy, E.A.; Awwad, N.S.; Ibrahim, H.A. Au@Ag core/shell nanoparticles prepared by laser-assisted method for optical limiting applications. *J. Mater. Sci. Mater. Electron.* **2021**, *32*, 14728–14739. [[CrossRef](#)]
16. Altowyan, A.S.; Mostafa, A.M.; Ahmed, H.A. Effect of liquid media and laser energy on the preparation of Ag nanoparticles and their nanocomposites with Au nanoparticles via laser ablation for optoelectronic applications. *Optik* **2021**, *241*, 167217. [[CrossRef](#)]
17. Mostafa, A.M.; Mwafy, E.A.; Awwad, N.S.; Ibrahim, H.A. Catalytic activity of Ag nanoparticles and Au/Ag nanocomposite prepared by pulsed laser ablation technique against 4-nitrophenol for environmental applications. *J. Mater. Sci. Mater. Electron.* **2021**, *32*, 11978–11988. [[CrossRef](#)]
18. Mostafa, A.M.; Mwafy, E.A.; Awwad, N.S.; Ibrahim, H.A. Synthesis of multi-walled carbon nanotubes decorated with silver metallic nanoparticles as a catalytic degradable material via pulsed laser ablation in liquid media. *Colloids Surf. A Physicochem. Eng. Asp.* **2021**, *626*, 126992. [[CrossRef](#)]
19. Mostafa, A.M.; Mwafy, E.A.; Lotfy, V.F.; Basta, A.H. Optical, electrical and mechanical studies of paper sheets coated by metals (Cu and Ag) via pulsed laser deposition. *J. Mol. Struct.* **2019**, *1198*, 126927. [[CrossRef](#)]
20. Mostafa, A.M.; Lotfy, V.F.; Mwafy, E.A.; Basta, A.H. Influence of coating by Cu and Ag nanoparticles via pulsed laser deposition technique on optical, electrical and mechanical properties of cellulose paper. *J. Mol. Struct.* **2020**, *1203*, 127472. [[CrossRef](#)]
21. Jelínek, M.; Kocourek, T.; Jurek, K.; Remsa, J.; Mikšovský, J.; Weiserová, M.; Strnad, J.; Luxbacher, T. Antibacterial properties of Ag-doped hydroxyapatite layers prepared by PLD method. *Appl. Phys. A* **2010**, *101*, 615–620. [[CrossRef](#)]
22. Pedarnig, J.D.; Heitz, J.; Stehrer, T.; Praher, B.; Viskup, R.; Siraj, K.; Moser, A.; Vlad, A.; Bodea, M.A.; Bäuerle, D.; et al. Characterization of nano-composite oxide ceramics and monitoring of oxide thin film growth by laser-induced breakdown spectroscopy. *Spectrochim. Acta Part B At. Spectrosc.* **2008**, *63*, 1117–1121. [[CrossRef](#)]
23. Mostafa, A.M.; Mwafy, E.A. Laser-assisted for preparation Ag/CdO nanocomposite thin film: Structural and optical study. *Opt. Mater.* **2020**, *107*, 110124. [[CrossRef](#)]
24. Mostafa, A.M.; Mwafy, E.A. Synthesis of ZnO/CdO thin film for catalytic degradation of 4-nitrophenol. *J. Mol. Struct.* **2020**, *1221*, 128872. [[CrossRef](#)]
25. Menazea, A.A.; Mostafa, A.M. Ag doped CuO thin film prepared via pulsed laser deposition for 4-nitrophenol degradation. *J. Environ. Chem. Eng.* **2020**, *8*, 104104. [[CrossRef](#)]

26. Srinivasan, N.; Kannan, J.C.; Satheeskumar, S. Examination of antibacterial properties of pure and aluminum doped zinc oxide nanoparticles. *Int. J. Chem. Tech. Res.* **2015**, *7*, 1708–1712.
27. Khatoon, U.T.; Rao, K.V.; Rao, J.R.; Aparna, Y. Synthesis and characterization of silver nanoparticles by chemical reduction method. In Proceedings of the International Conference on Nanoscience, Engineering and Technology (ICONSET 2011), Chennai, India, 28–30 November 2011; pp. 97–99.
28. Alkallas, F.H.; Ahmed, H.A.; Alrebdi, T.A.; Pashameah, R.A.; Alrefae, S.H.; Alsubhe, E.; Trabelsi, A.B.G.; Mostafa, A.M.; Mwafy, E.A. Removal of Ni(II) Ions by Poly(Vinyl Alcohol)/Al<sub>2</sub>O<sub>3</sub> Nanocomposite Film via Laser Ablation in Liquid. *Membranes* **2022**, *12*, 660. [[CrossRef](#)]
29. Alrebdi, T.A.; Ahmed, H.A.; Alkallas, F.H.; Mwafy, E.A.; Trabelsi, A.B.G.; Mostafa, A.M. Structural, linear and nonlinear optical properties of NiO nanoparticles–multi-walled carbon nanotubes nanocomposite for optoelectronic applications. *Radiat. Phys. Chem.* **2022**, *195*, 110088. [[CrossRef](#)]
30. Mostafa, A.M.; Mwafy, E.A.; Awwad, N.S.; Ibrahim, H.A. Linear and nonlinear optical studies of Ag/Zn/ZnO nanocomposite thin film prepared by pulsed laser deposition technique. *Radiat. Phys. Chem.* **2021**, *179*, 109233. [[CrossRef](#)]
31. Ahmad, M.; Ahmad, I.; Ahmed, E.; Akhtar, M.S.; Khalid, N.R. Facile and inexpensive synthesis of Ag doped ZnO/CNTs composite: Study on the efficient photocatalytic activity and photocatalytic mechanism. *J. Mol. Liq.* **2020**, *311*, 113326. [[CrossRef](#)]
32. Pimentel, A.; Araújo, A.; Coelho, B.; Nunes, D.; Oliveira, M.; Mendes, M.; Águas, H.; Martins, R.; Fortunato, E. 3D ZnO/Ag surface-enhanced Raman scattering on disposable and flexible cardboard platforms. *Materials* **2017**, *10*, 1351. [[CrossRef](#)]
33. Badawy, M.I.; Mahmoud, F.; Abdel-Khalek, A.A.; Gad-Allah, T.A.; Abdel Samad, A.A. Solar photocatalytic activity of sol–gel prepared Ag-doped ZnO thin films. *Desalinat. Water Treat.* **2014**, *52*, 2601–2608. [[CrossRef](#)]
34. Abozied, A.M.; Mostafa, A.M.; Abouelsayed, A.; Hassan, A.F.; Ramadan, A.A.; Al-Ashkar, E.A.; Anis, A. Preparation, characterization, and nonlinear optical properties of graphene oxide thin film doped with low chirality metallic SWCNTs. *J. Mater. Res. Technol.* **2021**, *12*, 1461–1472. [[CrossRef](#)]
35. Fageria, P.; Gangopadhyay, S.; Pande, S. Synthesis of ZnO/Au and ZnO/Ag nanoparticles and their photocatalytic application using UV and visible light. *Rsc Adv.* **2014**, *4*, 24962–24972. [[CrossRef](#)]
36. Ren, C.; Yang, B.; Wu, M.; Xu, J.; Fu, Z.; Guo, T.; Zhao, Y.; Zhu, C. Synthesis of Ag/ZnO nanorods array with enhanced photocatalytic performance. *J. Hazard. Mater.* **2010**, *182*, 123–129. [[CrossRef](#)]
37. Bahedi, K.; Addou, M.; El Jouad, M.; Sofiani, Z.; Alaoui Lamrani, M.; El Habbani, T.; Fellahi, N.; Bayoud, S.; Dghoughi, L.; Sahraoui, B.; et al. Diagnostic study of the roughness surface effect of zirconium on the third-order nonlinear-optical properties of thin films based on zinc oxide nanomaterials. *Appl. Surf. Sci.* **2009**, *255*, 4693–4695. [[CrossRef](#)]
38. Zhao, S.; Zhou, Y.; Zhao, K.; Liu, Z.; Han, P.; Wang, S.; Xiang, W.; Chen, Z.; Lü, H.; Cheng, B. Violet luminescence emitted from Ag-nanocluster doped ZnO thin films grown on fused quartz substrates by pulsed laser deposition. *Phys. B Condens. Matter* **2006**, *373*, 154–156. [[CrossRef](#)]
39. Khattab, T.A.; Gabr, A.M.; Mostafa, A.M.; Hamouda, T. Luminescent plant root: A step toward electricity-free natural lighting plants. *J. Mol. Struct.* **2019**, *1176*, 249–253. [[CrossRef](#)]
40. Alkallas, F.H.; Toghan, A.; Ahmed, H.A.; Alrefae, S.H.; Pashameah, R.A.; Alrebdi, T.A.; Mwafy, E.A.; Mostafa, A.M. Catalytic performance of NiO nanoparticles decorated carbon nanotubes via one-pot laser ablation method against methyl orange dye. *J. Mater. Res. Technol.* **2022**, *18*, 3336–3346. [[CrossRef](#)]
41. Altowyan, A.S.; Toghan, A.; Ahmed, H.A.; Pashameah, R.A.; Mwafy, E.A.; Alrefae, S.H.; Mostafa, A.M. Removal of methylene blue dye from aqueous solution using carbon nanotubes decorated by nickel oxide nanoparticles via pulsed laser ablation method. *Radiat. Phys. Chem.* **2022**, *198*, 110268. [[CrossRef](#)]
42. Mwafy, E.A.; Mostafa, A.M.; Awwad, N.S.; Ibrahim, H.A. Catalytic activity of multi-walled carbon nanotubes decorated with tungsten trioxides nanoparticles against 4-nitrophenol. *J. Phys. Chem. Solids* **2021**, *158*, 110258. [[CrossRef](#)]